Supporting Information

Intermetallic Pd_3Pb ultrathin nanoplate-constructed flowers with low-coordinated edge sites boost oxygen reduction performance

Sai Luo,[a] Yang Ou,[a] Lei Li,[a] Junjie Li,[a] Xingqiao Wu, Yi Jiang,[a] Mingxi Gao,[a] Xiaofang Yang,[b,] Hui Zhang,[a,*] Deren Yang[a]*

[a]State Key Laboratory of Silicon Materials, School of Materials Science and Engineering, Zhejiang University, Hangzhou, Zhejiang 310027, People's Republic of China. Email: msezhanghui@zju.edu.cn

[b]College of Materials Science and Engineering, Chongqing University, Chongqing 400044, People's Republic of China. Email: yangxf@cqu.edu.cn

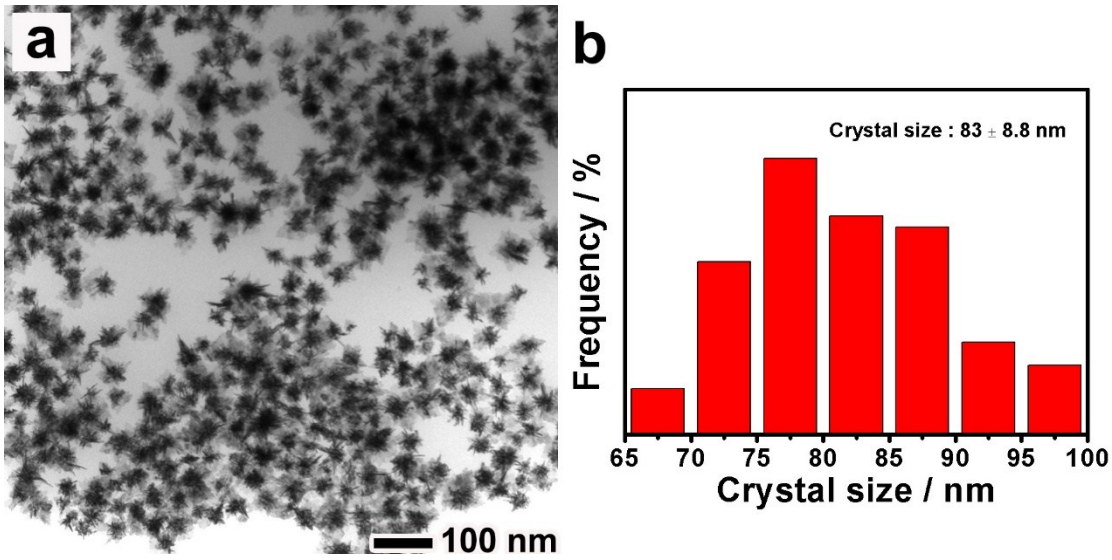

Figure S1. (a) Representative TEM images of the Pd_3Pb nanoflowers at low magnification and (b) the corresponding size distribution.

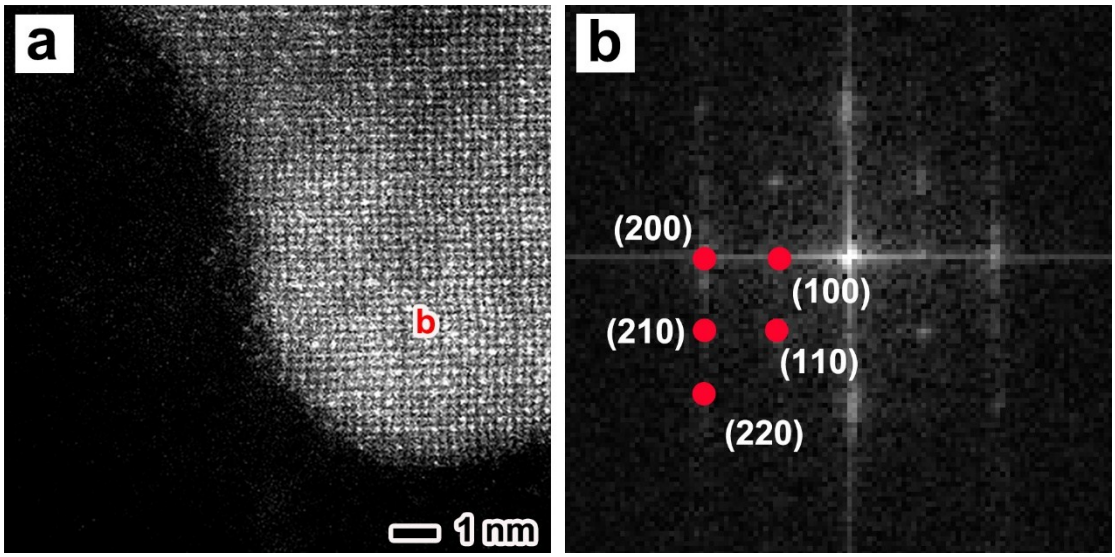

Figure S2. (a) HADDF-STTEM image of the Pd_3Pb nanoflowers at a higher magnification. (b) FFT pattern converted from the selected area in (a).

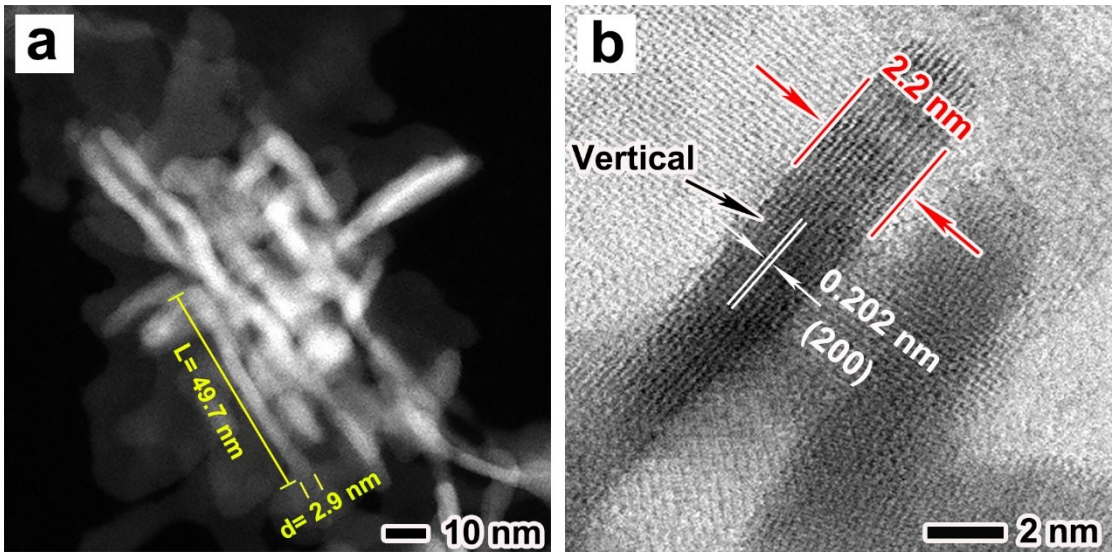

Figure S3. (a) HADDF image of the Pd_3Pb nanoflowers and (b) HRTEM image of the vertically upstanding nanoplates in the Pd_3Pb nanoflowers.

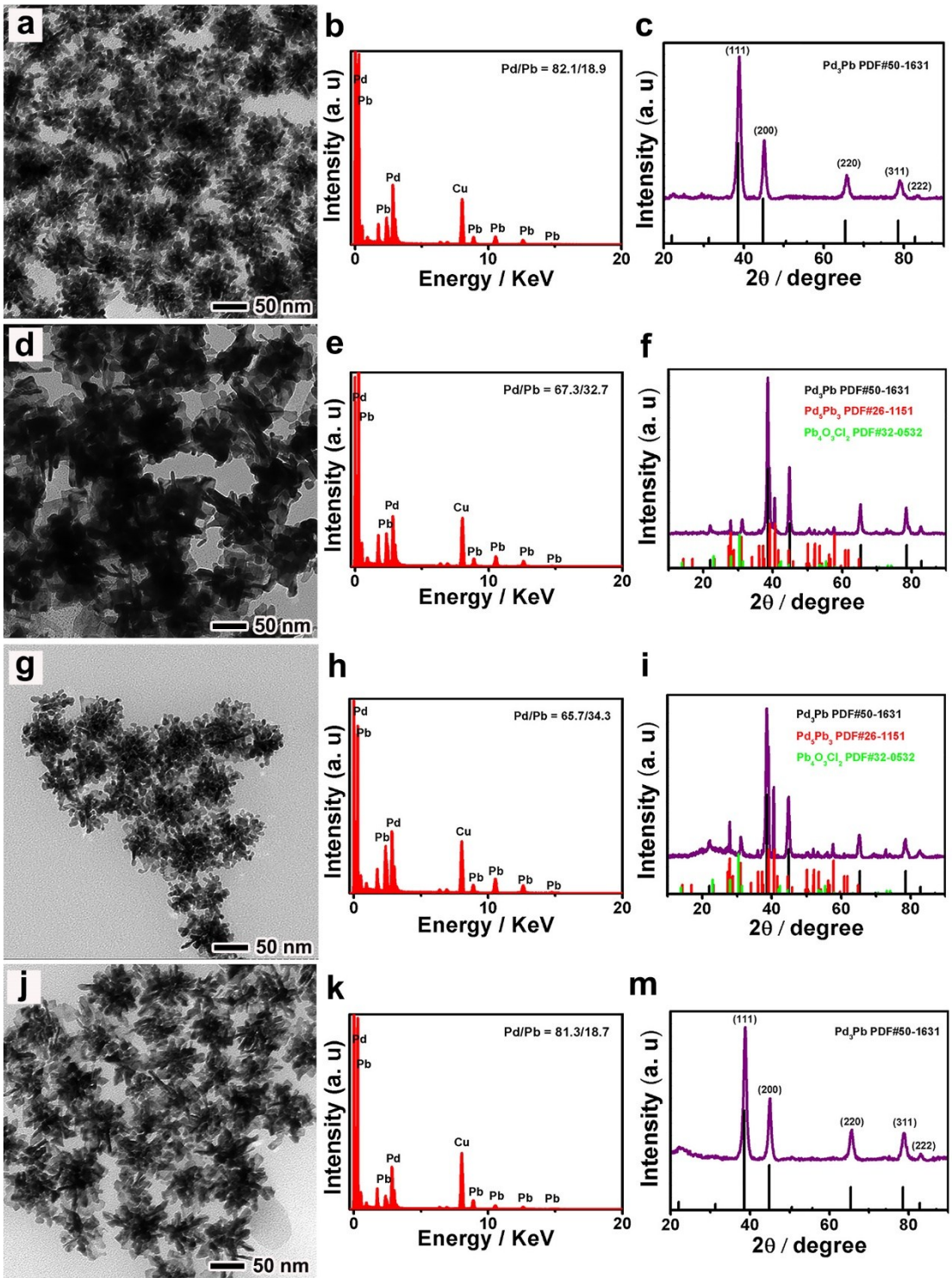

Figure S4. TEM images, EDX spectra and XRD patterns of the products prepared by using the starndard procedure except the use of (a, b, c) 0.12 mmol $Pd(acac)_2$ and 0.02 mmol $Pb(acac)_2$, (d, e, f) 0.03 mmol $Pd(acac)_2$ and 0.02 mmol $Pb(acac)_2$, (g, h, i) 0.06 mmol $Pd(acac)_2$ and 0.04 mmol $Pb(acac)_2$, and (j, k, m) 0.06 mmol $Pd(acac)_2$ and 0.01 mmol $Pb(acac)_2$.

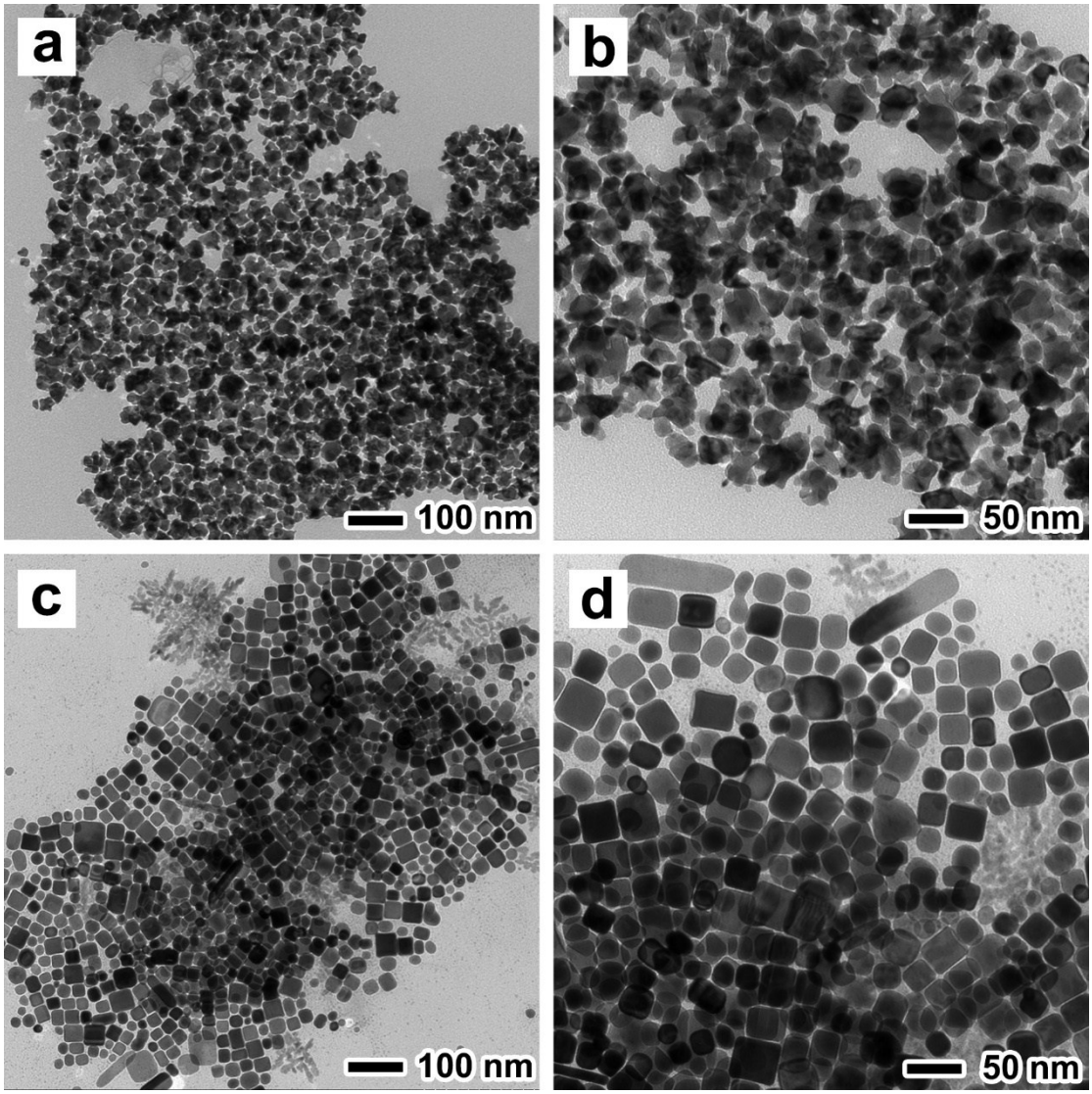

Figure S5. Representative TEM images of the products with the same conditions as those of Pd_3Pb nanoflowers but replacing 30 mg of AA with (a, b) 30 mg of glucose and (c, d) 30 mg of CA, respectively.

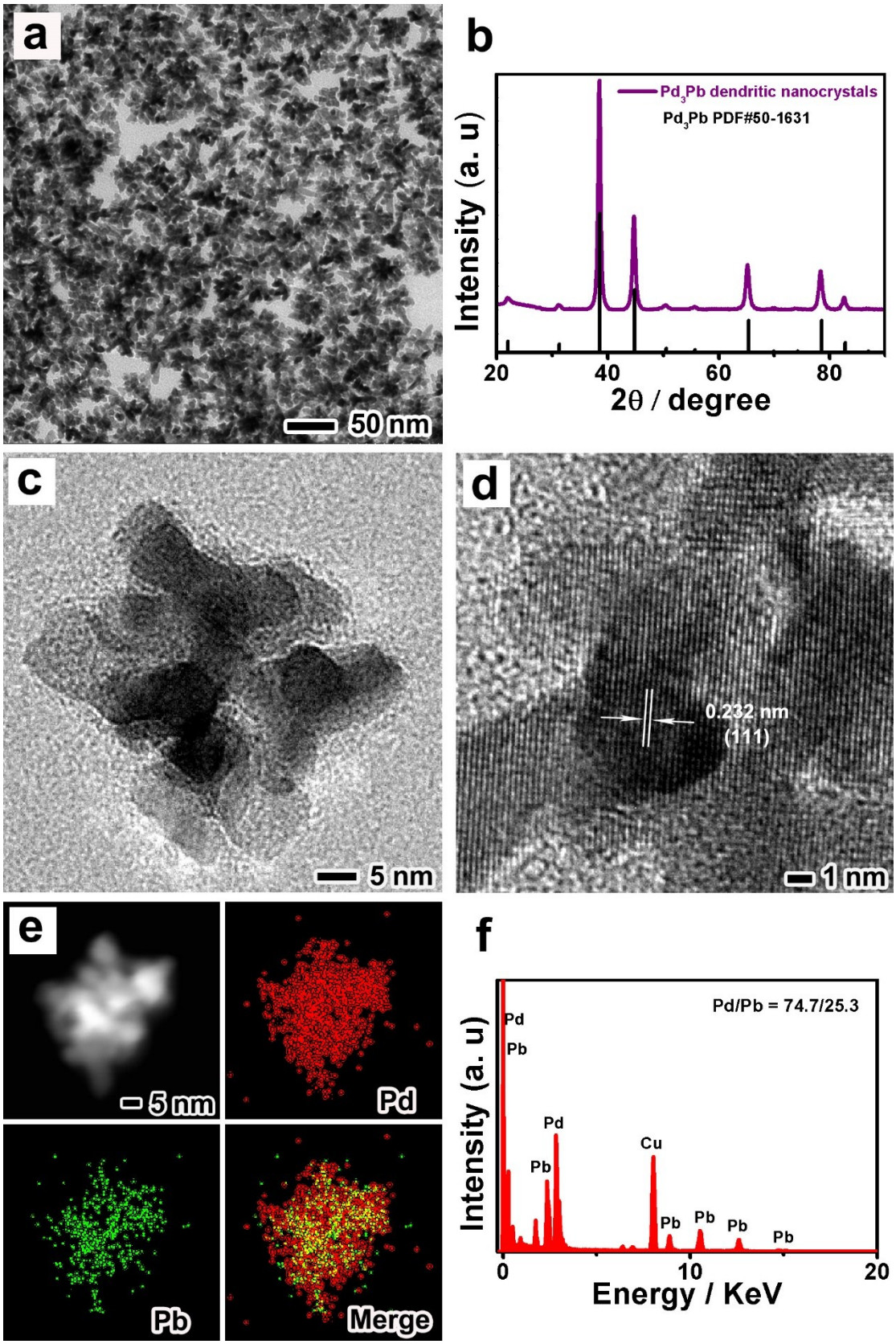

Figure S6. (a) TEM image, (b) XRD pattern, (c,d) HRTEM images, (e) EDX-mapping and (f) EDX spectrum of the Pd_3Pb dendritic nanocrystals prepared by using the starndard procedure for the synthesis of the Pd_3Pb nanoflowers in the absence of

CTAC.

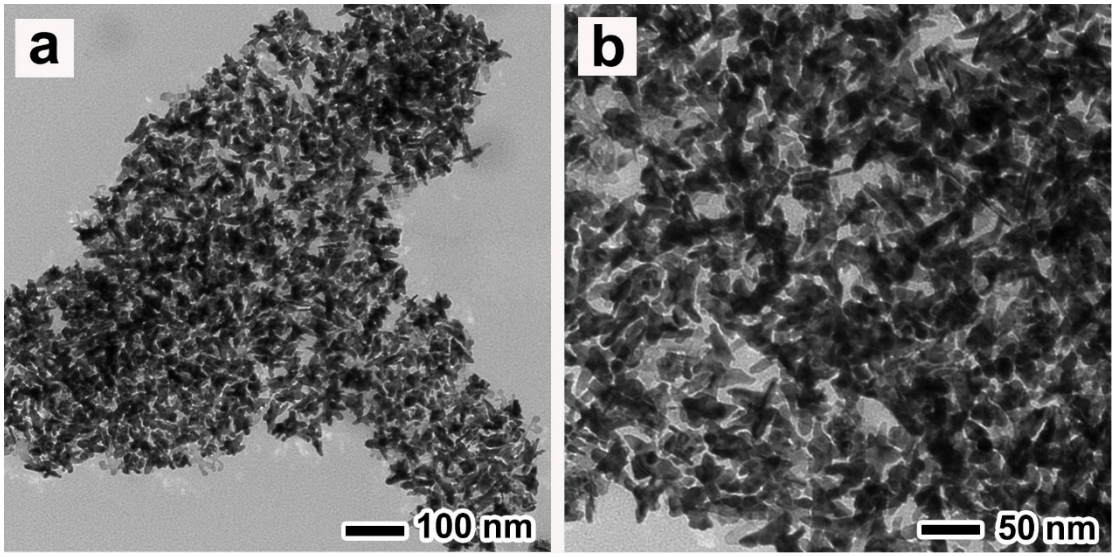

Figure S7. Representative TEM images of the products prepared by using the starndard procedure for the synthesis of the Pd_3Pb nanoflowers except for replacing 40 mg of CTAC with 40 mg of CTAB.

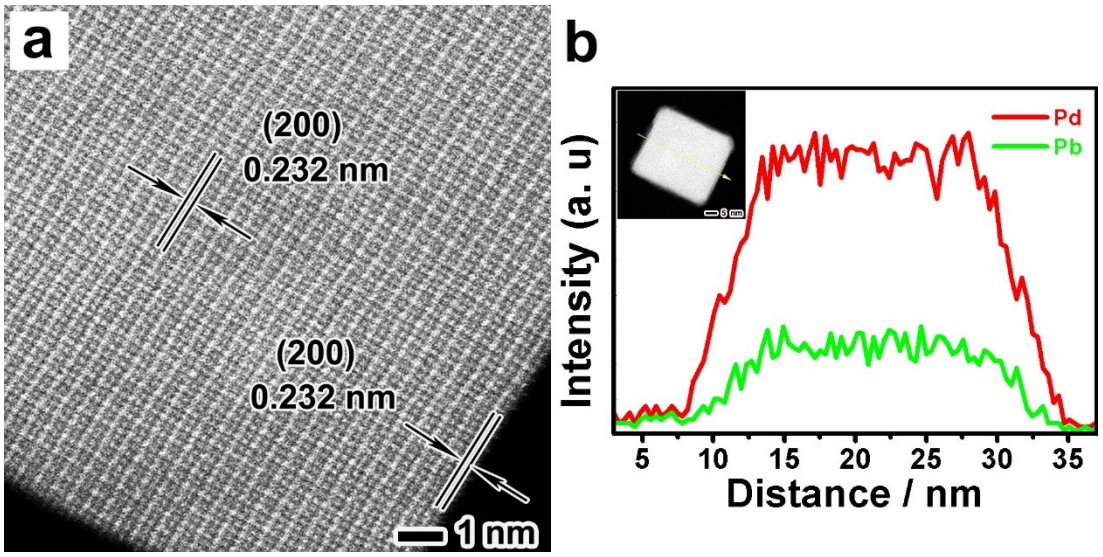

Figure S8. (a) Atomic-resolution HAADF-STEM image and (b) EDX line-scan profile of the Pd_3Pb nanocubes. The inset in (b) shows the corresponding HADDF-STEM images.

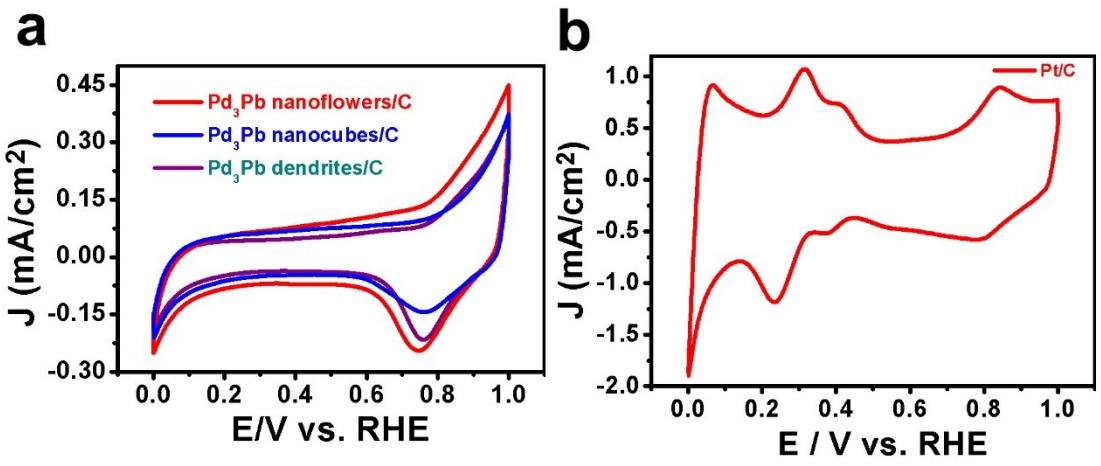

Figure S9. The cyclic voltammetry (CV) curves of (a) the Pd_3Pb nanoflowers/C, Pd_3Pb nanocubes/C and Pd_3Pb dendrites/C, and (b) commercial Pt/C in Ar-purged 0.1 M KOH solutions at a sweep rate of 50 mV/s.

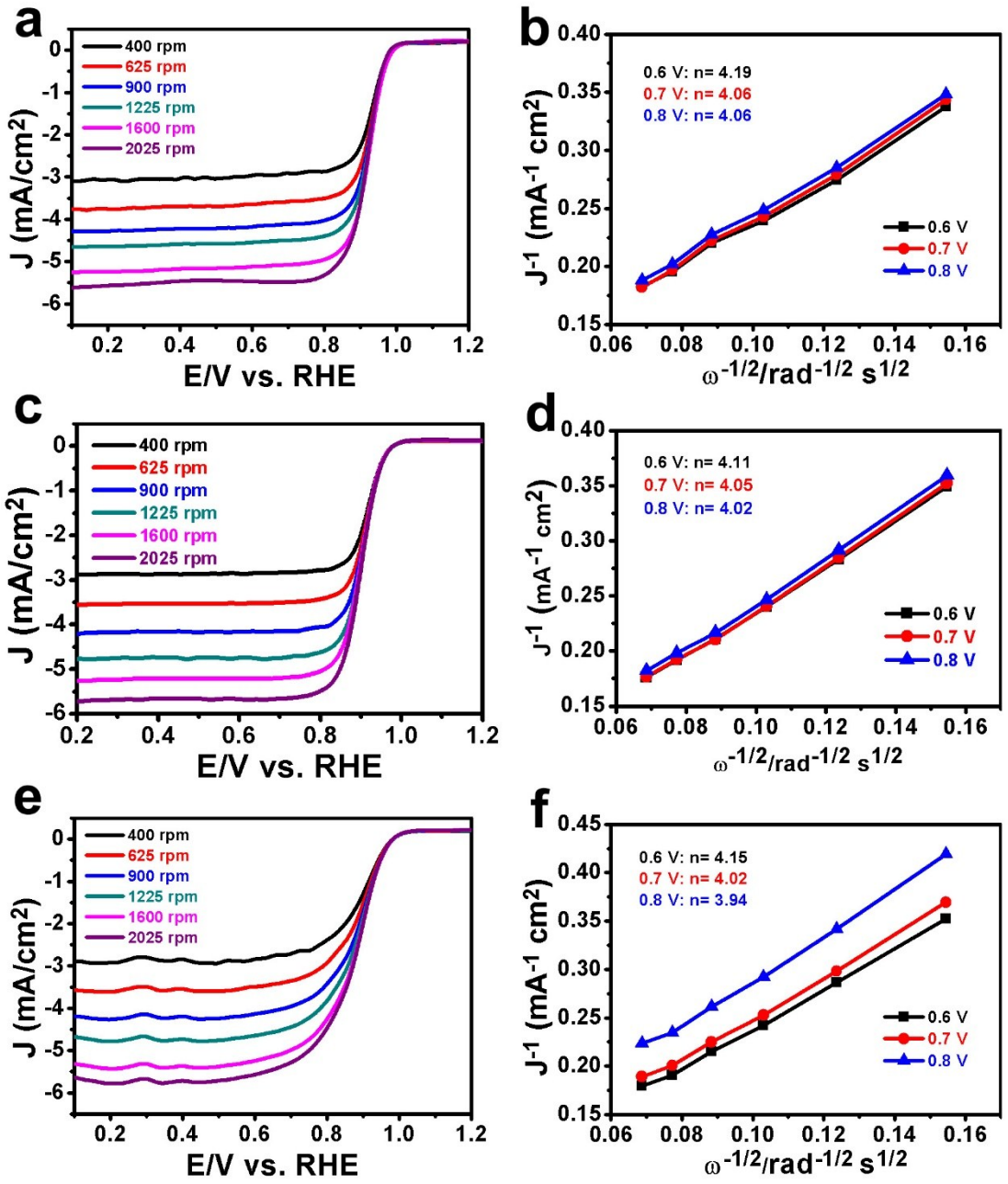

Figure S10. (a, c, e) Rotating-disk voltammograms of intermetallic Pd_3Pb nanocubes/C, Pd_3Pb dendrites/C and commercial Pt/C in O_2-saturated 0.1 M KOH at different rotation rates with a sweep rate of 10 mV s^{-1}. (b, d, f) The corresponding Koutechy-Levich plots of figure (a, c, e).

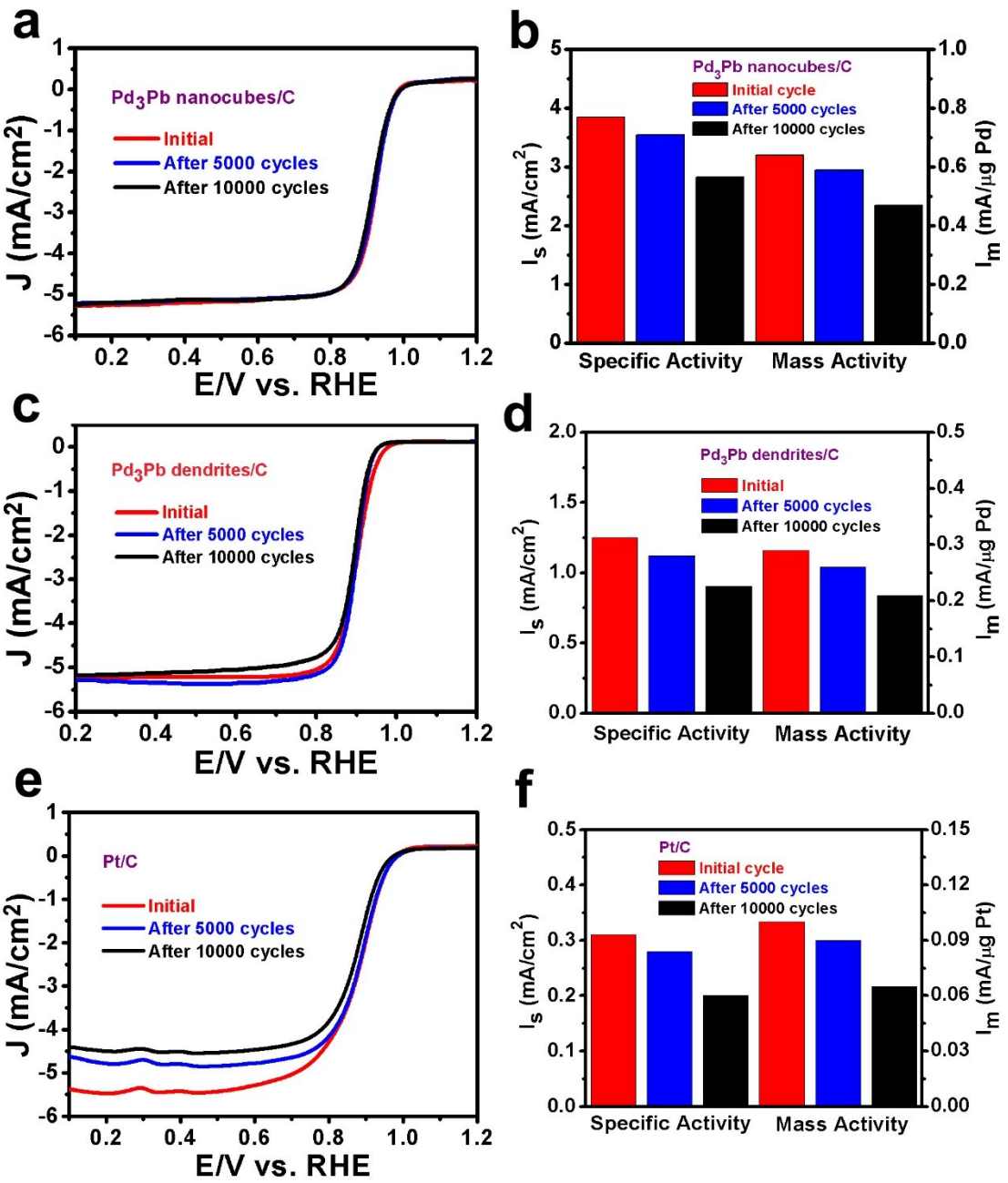

Figure S11. (a, c, e) ORR polarization curves of Pd_3Pb nanocubes/C, Pd_3Pb dendrites/C and commercial Pt/C in O_2-saturated 0.1 M KOH before and after different potential cycles between 0.6 and 1.0 V versus RHE, respectively. (b, d, f) The changes on specific and mass activities of the Pd_3Pb nanocubes/C and Pt/C after various potential cycles between 0.6 and 1.0 V versus RHE, respectively.

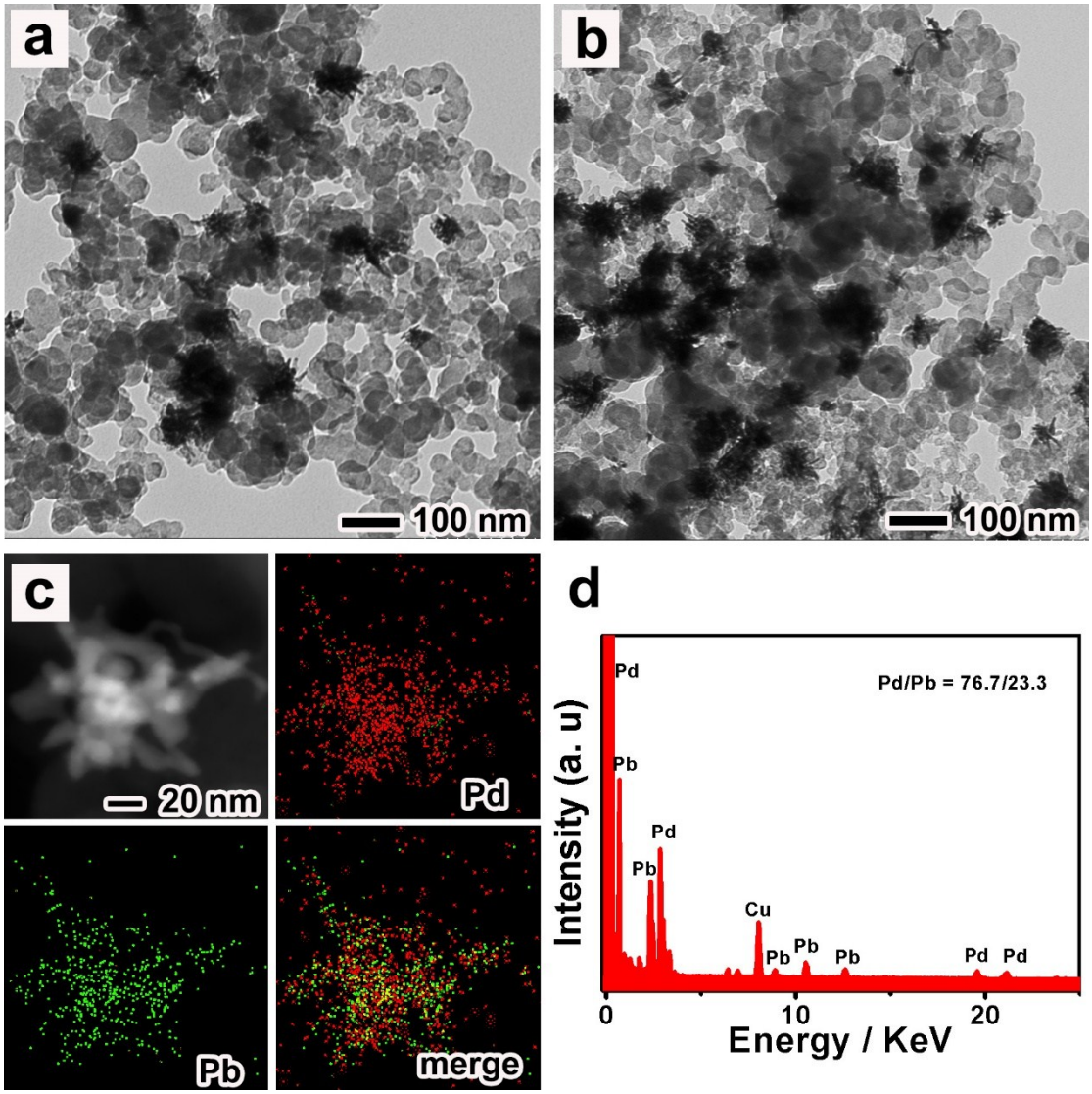

Figure S12. Representative TEM images of the Pd_3Pb nanoflowers/C (a) before and (b) after ADT. (c) HADDF-STEM-EDX mapping image and (d) EDX spectrum of the Pd_3Pb nanoflowers/C after 10000 cycles between 0.6 and 1.0 V versus RHE in O_2-saturated 0.1M KOH solution.

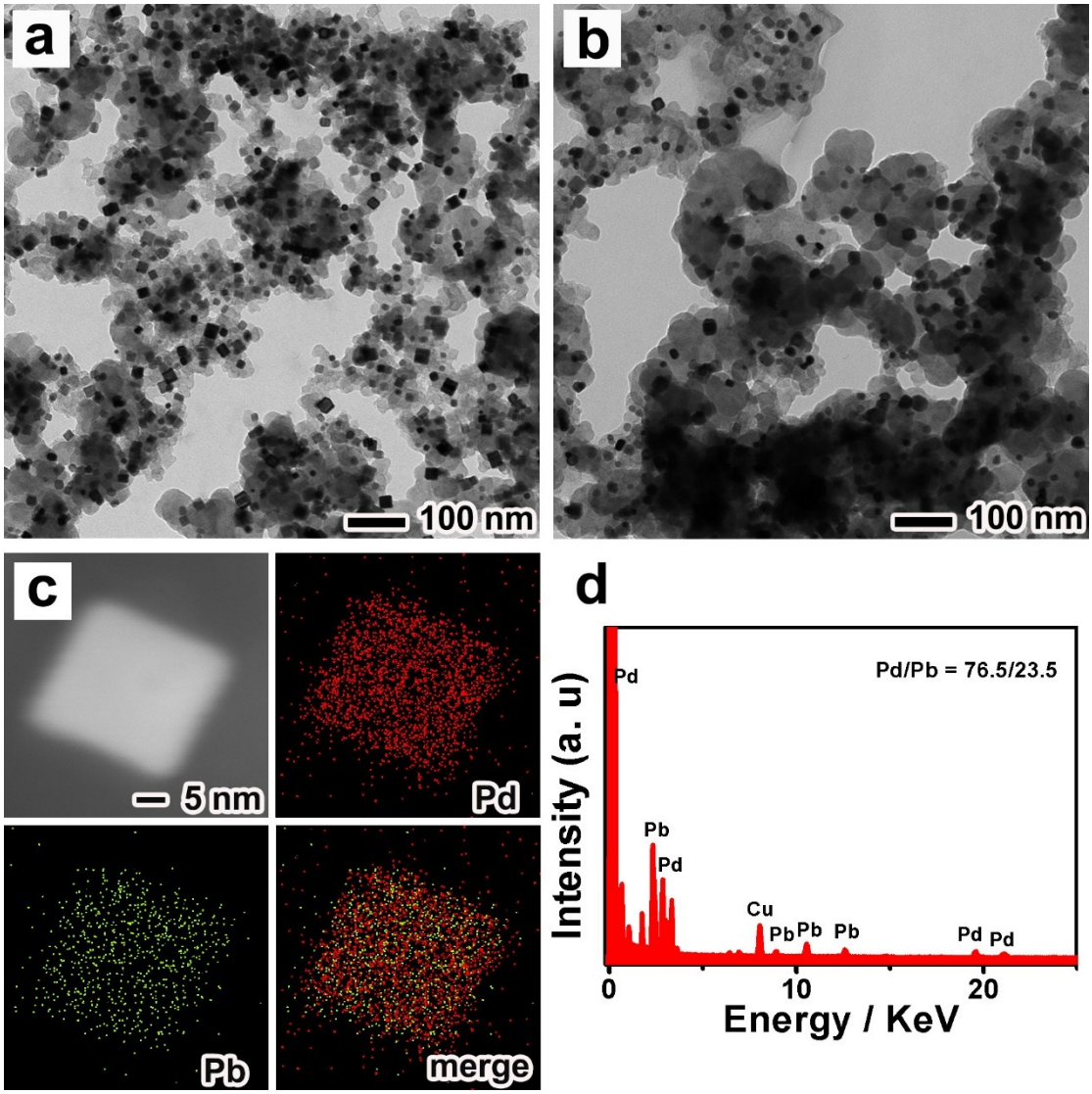

Figure S13. Representative TEM images of the intermetallic Pd_3Pb nanocubes/C (a) before and (b) after ADT. (c) HADDF-STEM-EDX mapping image and (d) EDX spectrum of the intermetallic Pd_3Pb nanocubes after 10000 cycles between 0.6 and 1.0 V versus RHE in O_2-saturated 0.1M KOH solution.

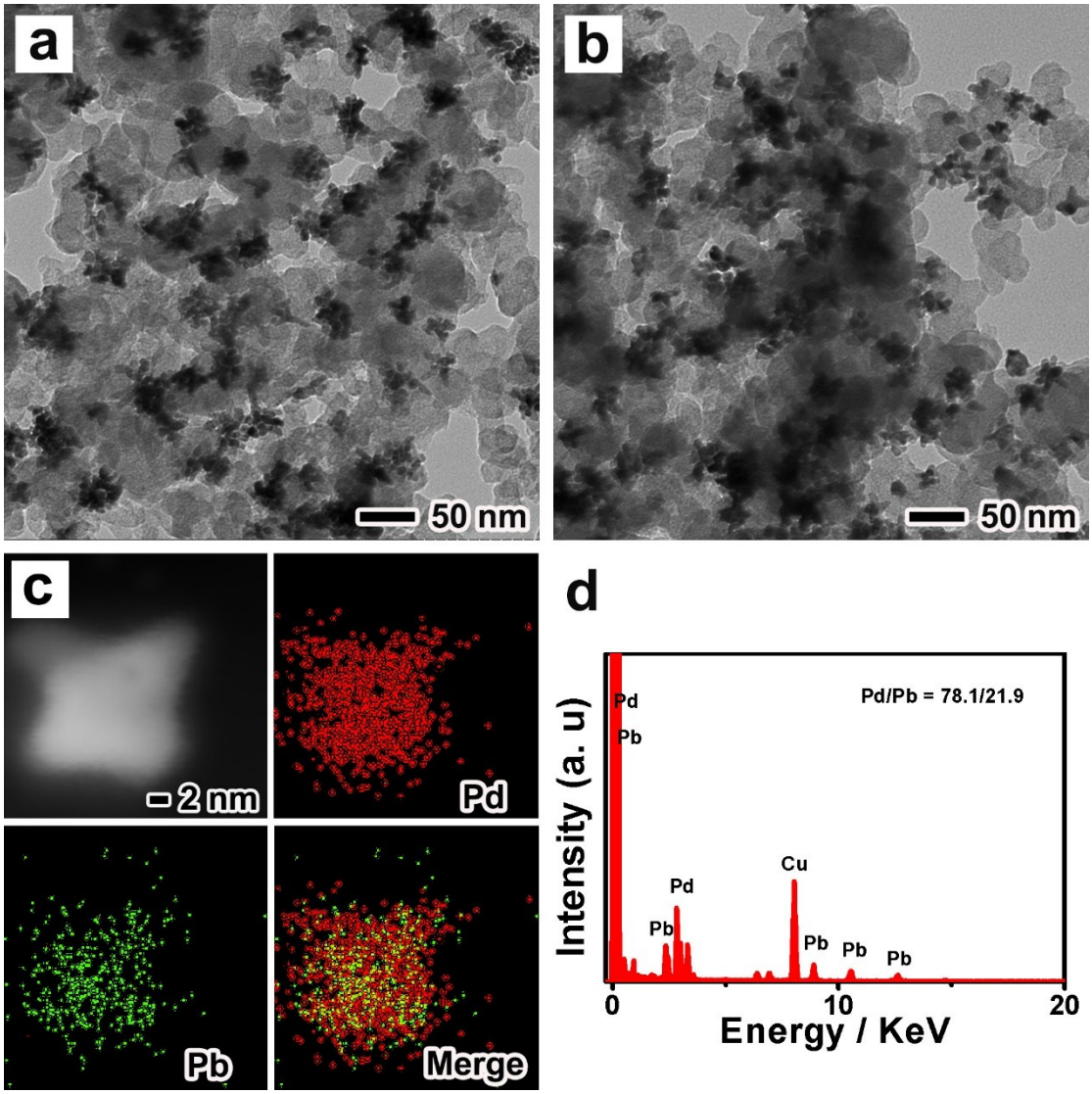

Figure S14. Representative TEM images of the intermetallic Pd_3Pb dendrites/C (a) before and (b) after ADT. (c) HADDF-STEM-EDX mapping image and (d) EDX spectrum of the intermetallic Pd_3Pb dendrites after 10000 cycles between 0.6 and 1.0 V versus RHE in O_2-saturated 0.1M KOH solution.

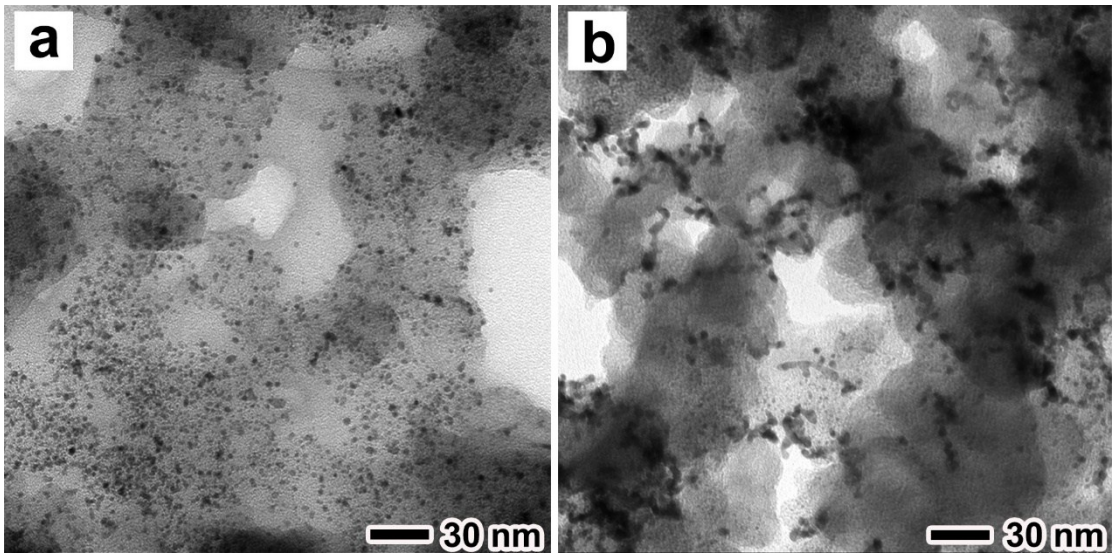

Figure S15. Representative TEM images of the commercial Pt/C (a) before and (b) after 10000 potential cycles between 0.6 and 1.0 V versus RHE in O_2-saturated 0.1M KOH solution.

Table S1. ORR mass activities at 0.9 V vs. RHE in 0.1 M KOH of the Pd_3Pb nanoflowers/C in this work and various excellent Pd-based nanocatalysts recorded in the literatures to date. (NA: Not available)

No.	Catalysts	Mass activities ($mA/\mu g_{Pd}$)	Specific Activities (mA/cm^2)	Reference
1	**Pd_3Pb nanoflowers/C**	**1.14**	**4.47**	**This work**
2	Pd_3Pb nanoplates	0.78	NA	Ref. 1
3	Pd_3Pb nanowire networks	0.61	15.7	Ref. 2
4	Pd_3Pb tripods	0.56	1.76	Ref. 3
5	Ordered Pd_3Pb/C	0.1689	NA	Ref. 4
6	Ordered Pd_3Fe/C	0.0974	NA	Ref. 5
7	PdCuCo NPs/C-375 ^oC	0.13	NA	Ref. 6
8	$Pd/W_{18}O_{49}$ hybrids	0.216	0.45	Ref. 7
9	AuPdCo/C intermetallic	0.13	NA	Ref. 8
10	PdCu tetrapods	0.29	0.73	Ref. 9
11	Pd_6Ni icosahedra	0.22	0.66	Ref. 10
12	$Ni@Pd_3$/C	0.038	0.13	Ref. 11
13	Pd_4Fe nanoflowers/C	0.975	2.78	Ref. 12

(1) K. Wang, Y. Qin, F. Lv, M. Li, Q. Liu, F. Lin, J. Feng, C. Yang, P. Gao, and S. Guo, *Small Methods,* 2018, **2,** 1700331.

(2) Q. Shi, C. Zhu, C. Bi, H. Xia, M. Engelhard, D. Du, and Y. Lin, *J. Mater. Chem. A,* 2017, **5,** 23952-23959.

(3) L. Bu, Q. Shao, Y. Pi, J. Yao, M. Luo, J. Lang, S. Hwang, H. Xin, B. Huang, J. Guo, D. Su, S. Guo, and X. Huang, *Chem,* 2018, **4,** 359-371.

(4) Z. Cui, H. Chen, M. Zhao, and F. DiSalvo, *Nano Lett.,* 2016, **16,** 2560-2566.

(5) Z. Cui, L. Li, A. Manthiram, and J. Goodenough, *J. Am. Chem. Soc.,* 2015, **137,** 7278-7281.

(6) K. Jiang, P. Wang, S. Guo, X. Zhang, X. Shen, G. Lu, D. Su, and X. Huang, *Angew. Chem. Int. Ed.,* 2016, **55,** 9030-9035.

(7) Y. Lu, Y. Jiang, X. Gao, X. Wang, and W. Chen, *J. Am. Chem. Soc.,* 2014, **136,**

11687-11697.

(8) K. Kuttiyiel, K. Sasaki, D. Su, L. Wu, Y. Zhu & R. Adzic, *Nat. Commun.,* 2014, **5,** 5185.

(9) L. Zhang, S. Chen, Y. Dai, Z. Shen, M. Wei, R. Huang, H. Li, T. Zheng, Y. Zhang, S. Zhou, and J. Zeng, *ChemCatChem,* 2018, **10,** 925-930.

(10) Y. Feng, Q. Shao, Y. Ji, X. Cui, Y. Li, X. Zhu, X. Huang, *Sci. Adv.,* 2018, **4,** 8817

(11) J. Jiang, H. Gao, S. Lu, X. Zhang, C. Wang, W. Wang, and H. Yu, *J. Mater. Chem. A,* 2017, **5,** 9233-9240.

(12) C. Lian, Y. Cheng, L. Chen, X. Han, X. Lei, Y. Liu, and Y. Wang, *Chem. Commun.,* 2018, **54,** 7058-7061.